
Research Article: New Research | Cognition and Behavior

Idiosyncratic, retinotopic bias in face identification modulated by familiarity

Matteo Visconti di Oleggio Castello¹, Morgan Taylor¹, Patrick Cavanagh^{1,2} and M. Ida Gobbini^{1,3}

¹*Department of Psychological & Brain Sciences, Dartmouth College, 03755, Hanover, NH, USA*

²*Department of Psychology, Glendon College, M4N 3M6, Toronto, ON, Canada*

³*Dipartimento di Medicina Specialistica, Diagnostica, e Sperimentale, University of Bologna, 40100, Bologna, Italy*

DOI: 10.1523/ENEURO.0054-18.2018

Received: 2 February 2018

Revised: 25 July 2018

Accepted: 21 August 2018

Published: 1 October 2018

Author Contributions: M.V.D.O.C., P.C., and M.I.G. designed research; M.V.D.O.C. and M.K.T. performed research; M.V.D.O.C. analyzed data; M.V.D.O.C. and M.I.G. wrote the paper.

The authors declare no competing financial interests.

Correspondence: M. Ida Gobbini, mariaida.gobbini@unibo.it or Matteo Visconti di Oleggio Castello, mvdoc.gr@dartmouth.edu

Cite as: eNeuro 2018; 10.1523/ENEURO.0054-18.2018

Alerts: Sign up at eneuro.org/alerts to receive customized email alerts when the fully formatted version of this article is published.

Accepted manuscripts are peer-reviewed but have not been through the copyediting, formatting, or proofreading process.

1 **Idiosyncratic, retinotopic bias in face identification**
2 **modulated by familiarity**

3 Abbreviated title: Retinotopic bias in face identification

4 Matteo Visconti di Oleggio Castello^{1,*}, Morgan Taylor¹, Patrick Cavanagh^{1,2},
5 M. Ida Gobbini^{1,3,*}

6 ¹Department of Psychological & Brain Sciences,
7 Dartmouth College,
8 Hanover NH, 03755, USA

9 ²Department of Psychology
10 Glendon College
11 Toronto ON, M4N 3M6 Canada

12 ³Dipartimento di Medicina Specialistica, Diagnostica, e Sperimentale,
13 University of Bologna,
14 40100 Bologna, Italy

15 *corresponding authors:

16 M. Ida Gobbini, mariaida.gobbini@unibo.it

17 Matteo Visconti di Oleggio Castello, mvdoc.gr@dartmouth.edu

18 6207 Moore Hall

19 Dartmouth College

20 Hanover, NH 03755, USA

21

22 Number of pages: 50

23 Number of figures: 5

24 Number of tables: 3

25 Words (Abstract): 169

26 Words (Introduction): 1,021

27 Words (Discussion): 2,090

28

29 **Conflict of Interest**

30 The authors declare no competing financial interests.

31

32 **Acknowledgments**

33 We would like to thank Carlo Cipolli for helpful discussions. We would like to thank
34 the Martens Family Fund and Dartmouth College for their support.

35 **Abstract**

36 The perception of gender and age of unfamiliar faces is reported to vary
37 idiosyncratically across retinal locations such that, for example, the same androgynous
38 face may appear to be male at one location but female at another. Here we test spatial
39 heterogeneity for the recognition of the *identity* of personally familiar faces in human
40 participants. We found idiosyncratic biases that were stable within participants and
41 that varied more across locations for low as compared to high familiar faces. These
42 data suggest that like face gender and age, face identity is processed, in part, by
43 independent populations of neurons monitoring restricted spatial regions and that the
44 recognition responses vary for the same face across these different locations.
45 Moreover, repeated and varied social interactions appear to lead to adjustments of
46 these independent face recognition neurons so that the same familiar face is
47 eventually more likely to elicit the same recognition response across widely separated
48 visual field locations. We provide a mechanistic account of this reduced retinotopic
49 bias based on computational simulations.

50 **Significance statement**

51 In this work we tested spatial heterogeneity for the recognition of personally familiar
52 faces. We found retinotopic biases that varied more across locations for low as

53 compared to highly familiar faces. The retinotopic biases were idiosyncratic and stable
54 within participants. Our data suggest that, like face gender and age, face identity is
55 processed by independent populations of neurons monitoring restricted spatial
56 regions and that recognition may vary for the same face at these different locations.
57 Unlike previous findings, our data and computational simulation address the effects
58 of learning and show how increased familiarity modifies the representation of face
59 identity in face-responsive cortical areas. This new perspective has broader
60 implications for understanding how learning optimizes visual processes for socially
61 salient stimuli.

62 **Introduction**

63 We spend most of our days interacting with acquaintances, family and close friends.
64 Because of these repeated and protracted interactions, the representation of
65 personally familiar faces is rich and complex, as reflected by stronger and more
66 widespread neural activation in the distributed face processing network, as compared
67 to responses to unfamiliar faces (Gobbini and Haxby, 2007; Taylor et al., 2009;
68 Gobbini, 2010; Natu and O'Toole, 2011; Bobes et al., 2013; Sugiura, 2014; Ramon and
69 Gobbini, 2017; Visconti di Oleggio Castello et al., 2017a). Differences in
70 representations are also reflected in faster detection and more robust recognition of
71 familiar faces (Burton et al., 1999; Gobbini et al., 2013; Ramon et al., 2015; Visconti

72 di Oleggio Castello and Gobbini, 2015; Guntupalli and Gobbini, 2017; Visconti di
73 Oleggio Castello et al., 2017b).

74 The advantage for familiar faces could originate at different stages of the face
75 processing system. The classic psychological model by Bruce and Young (1986) posits
76 that recognition of familiar faces occurs when the structural encoding of a perceived
77 face matches stored representations (Bruce and Young, 1986). In this model the stored
78 representations of familiar faces consist of “an interlinked set of expression-
79 independent structural codes for distinct head angles, with some codes reflecting the
80 global configuration at each angle and others representing particular distinctive
81 features” (Bruce and Young, 1986, p. 309). Behavioral evidence supports the
82 hypothesis that local features are processed differentially for personally familiar faces.
83 For example, in a study of perception of gaze direction and head angle, changes in eye
84 gaze were detected around 100ms faster in familiar than in unfamiliar faces (Visconti
85 di Oleggio Castello and Gobbini, 2015). In another study, the advantage for personally
86 familiar faces was maintained after face inversion, a manipulation that is generally
87 thought to reduce holistic processing in favor of local processing (Visconti di Oleggio
88 Castello et al., 2017b).

89 Taken together, these results suggest that optimized processing of personally familiar
90 faces could rely on local features. This could be sufficient to initially drive a
91 differential response to personally familiar faces. In a study measuring saccadic

92 reaction time, correct and reliable saccades to familiar faces were recorded as fast as
93 180 ms when unfamiliar faces were distractors (Visconti di Oleggio Castello and
94 Gobbini, 2015). In an EEG study using multivariate analyses, significant decoding of
95 familiarity could be detected at around 140 ms from stimulus onset (Barragan-Jason
96 et al., 2015). At such short latencies it is unlikely that a viewpoint-invariant
97 representation of an individual face's identity drives these differential responses. To
98 account for facilitated, rapid detection of familiarity, we have previously
99 hypothesized that personally familiar faces may be recognized quickly based on
100 diagnostic, idiosyncratic features, which become highly learned through extensive
101 personal interactions (Visconti di Oleggio Castello and Gobbini, 2015; Visconti di
102 Oleggio Castello et al., 2017b). Detection of these features may occur early in the face-
103 processing system, allowing an initial, fast differential processing for personally
104 familiar faces.

105 Processes occurring at early stages of the visual system can show idiosyncratic
106 retinotopic biases (Greenwood et al., 2017). Afraz et al. (2010) reported retinotopic
107 biases for perceiving face gender and age that varied depending on stimulus location
108 in the visual field and were specific to each subject. These results suggest that
109 diagnostic facial features for gender and age are encoded in visual areas with limited
110 position invariance. Neuroimaging studies have shown that face-processing areas such
111 as OFA, pFus, and mFus have spatially restricted population receptive fields that

112 could result in retinotopic differences (Kay et al., 2015; Silson et al., 2016; Grill-
113 Spector et al., 2017b). In addition, local facial features activate the OFA (and the
114 putative monkey homologue PL, see Issa and DiCarlo, 2012): responses to face parts
115 are stronger when they are presented in typical locations (de Haas et al., 2016), and
116 population activity in the OFA codes the position and relationship between face parts
117 (Henriksson et al., 2015).

118 Here we hypothesized that detectors of diagnostic visual features that play a role in
119 identification of familiar faces may also show idiosyncratic retinotopic biases and that
120 these biases may be tuned by repeated interactions with personally familiar faces.
121 Such biases may affect recognition of the identities presented in different parts of the
122 visual field and may be modulated by the familiarity of those identities. We tested
123 this hypothesis by presenting participants with morphed stimuli of personally familiar
124 individuals that were briefly shown at different retinal locations. In two separate
125 experiments we found that participants showed idiosyncratic biases for specific
126 identities in different visual field locations, and these biases were stable on retesting
127 after weeks. Importantly, the range of the retinal biases was inversely correlated with
128 the reported familiarity of each target identity, suggesting that prolonged personal
129 interactions with the target individuals reduced retinal biases.

130 We hypothesized that these biases could arise because neurons in face-processing
131 areas have restricted receptive fields centered around the fovea (Afraz et al., 2010;

132 Kay et al., 2015; Silson et al., 2016), resulting in an incomplete coverage of the visual
133 field. Thus, identifying a particular face at different peripheral locations would rely
134 on independent populations tuned to that face that cover a limited portion of the
135 visual field biased toward the foveal region, leading to variations in identification
136 across locations. To test this mechanism, we created a computational simulation in
137 which increased familiarity with a specific identity resulted in changes of neural
138 properties of the units responsive to that particular face. By either increasing the
139 number of units responsive to a face or by increasing the receptive field size of those
140 units, this simple learning mechanism accounted for the reduced biases reported in
141 the two experiments, providing testable hypotheses for future work.

142 These findings support the hypothesis that asymmetries in the processing of
143 personally familiar faces can arise at stages of the face-processing system where there
144 is reduced position invariance and where local features are being processed, such as
145 in OFA or perhaps even earlier. Our behavioral results show that prolonged, personal
146 interactions can modify the neural representation of faces at this early level of
147 processing, and our computational simulation provides a simple account of how this
148 learning process can be implemented at the neural level.

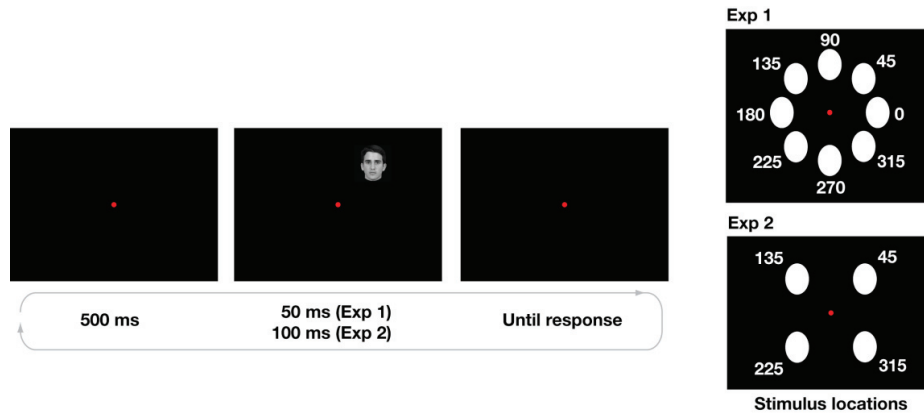
149 **Materials and Methods**

Figure 1. Experimental paradigm. The left panel shows an example of the experimental paradigm, while the right panel shows the locations used in Experiment 1 (eight locations, top panel) and in Experiment 2 (four locations, bottom panel).

150 **Stimuli**

151 Pictures of the faces of individuals who were personally familiar to the participants
 152 (graduate students in the same department) were taken in a photo studio room with
 153 the same lighting condition and the same camera. Images of two individuals were used
 154 for Experiment 1, and images of three individuals were used for Experiment 2. All
 155 individuals portrayed in the stimuli signed written informed consent for the use of
 156 their pictures for research and in publications.

157 The images were converted to grayscale, resized and centered so that the eyes were
 158 aligned in the same position for the three identities, and the background was manually
 159 removed. These operations were performed using ImageMagick and Adobe

160 Photoshop CS4. The resulting images were matched in luminance (average pixel
161 intensity) using the SHINE toolbox (function *lumMatch*) (Willenbockel et al., 2010)
162 after applying an oval mask, so that only pixels belonging to the face were modified.
163 The luminance-matched images were then used to create morph continua (between
164 two identities in Experiment 1, see Figure 2; and among three identities in Experiment
165 2, see Figure 3) using Abrosoft Fantamorph (v. 5.4.7) with seven percentages of
166 morphing: 0, 17, 33, 50, 67, 83, 100 (see Figures 2, 3).

167 ***Experiment 1***

168 *Paradigm*

169 The experimental paradigm was similar to that by Afraz et al., (2010). In every trial
170 participants would see a briefly flashed image in one of eight locations at the
171 periphery of their visual field (see Figure 1). Each image was shown for 50 ms at a
172 distance of 7° of visual angle from the fixation point, and subtended approximately
173 4° x 4° of visual angle. The images could appear in one of eight locations evenly spaced
174 by 45 angular degrees around fixation. For Experiment 1, only the morph *ab* was used
175 (see Figure 1). Participants were required to maintain fixation on a central red dot
176 subtending approximately 1° of visual angle.

177 After the image disappeared, participants reported which identity they saw using the
178 left (identity *a*) and right (identity *b*) arrow keys. There was no time limit for

179 responding, and participants were asked to be as accurate as possible. After
180 responding, participants had to press the spacebar key to continue to the next trial.

181 Participants performed five blocks containing 112 trials each, for a total of 560 trials.
182 In each block all the images appeared twice for every angular location (8 angular
183 locations \times 7 morph percentages \times 2 = 112). This provided ten data points for each
184 percentage morphing at each location, for a total of 70 trials at each angular location.

185 Before the experimental session participants were shown the identities used in the
186 experiment (corresponding to 0% and 100% morphing, see Figure 2), and practiced
187 the task with 20 trials. These data were discarded from the analyses. Participants
188 performed two identical experimental sessions at least four weeks apart.

189 Participants sat at a distance of approximately 50 cm from the screen, with their chin
190 positioned on a chin-rest. The experiment was run using Psychtoolbox (Kleiner et al.,
191 2007) (version 3.0.12) in MATLAB (R2014b). The screen operated at a resolution of
192 1920x1200 and a 60Hz refresh rate.

193 *Subjects*

194 We recruited six subjects for this experiment (three males, including one of the
195 authors, MVdOC). The sample size for Experiment 1 was not determined by formal
196 estimates of power, and was limited by the availability of participants familiar with
197 the stimulus identities. After the first experimental session, two participants (one

198 male, one female) were at chance level in the task, thus only data from four subjects
199 (two males, mean age 27.50 ± 2.08 SD) were used for the final analyses.

200 All subjects had normal or corrected-to-normal vision, and provided written
201 informed consent to participate in the experiment. The study was approved by the
202 Dartmouth College Committee for the Protection of Human Subjects.

203 ***Experiment 2***

204 *Paradigm*

205 Experiment 2 differed from Experiment 1 in the following parameters (see Figures 1,
206 3): 1. three morph continua (*ab*, *ac*, *bc*) instead of one; 2. images appeared in four
207 locations (45° , 135° , 225° , 315°) instead of eight; 3. images were shown for 100 ms
208 instead of 50 ms to make the task easier.

209 All other parameters were the same as in Experiment 1. Participants had to indicate
210 which of the three identities they saw by pressing the left (identity *a*), right (identity
211 *b*), or down (identity *c*) arrow keys.

212 Participants performed ten blocks containing 84 trials each, for a total of 840 trials. In
213 each block all the images appeared once for every angular location (4 angular locations
214 x 7 morph percentages x 3 morphs = 84). We used 70 data points at every angular
215 location to fit the model for each pair of identities. Thus, we used the responses to

216 different unmorphed images for each pair of identities, ensuring independence of the
217 models.

218 Before the experimental session participants were shown the identities used in the
219 experiment (corresponding to 0% and 100% morphing, see Figure 3), and practiced
220 the task with 20 trials. These data were discarded from the analyses. Participants
221 performed two experimental sessions at least four weeks apart.

222 *Subjects*

223 Ten participants (five males, mean age 27.30 ± 1.34 SD) participated in Experiment 2,
224 five of which were recruited for Experiment 1 as well. No authors participated in
225 Experiment 2. The sample size ($n = 10$) was determined using G*Power3 (Faul et al.,
226 2007, 2009) to obtain 80% power at $\alpha = 0.05$ based on the correlation of the PSE
227 estimates across sessions in Experiment 1, using a bivariate normal model (one-tailed).

228 All subjects had normal or corrected-to-normal vision, and provided written
229 informed consent to participate in the experiment. The study was approved by the
230 Dartmouth College Committee for the Protection of Human Subjects.

231 *Familiarity and contact scales*

232 After the two experimental sessions, participants completed a questionnaire designed
233 to assess how familiar each participant was with the identities shown in the
234 experiment. Participants saw each target identity, and were asked to complete various

235 scales for that identity. The questionnaire comprised the “Inclusion of the Other in
236 the Self” scale (IOS) (Aron et al., 1992; Gächter et al., 2015), the “Subjective Closeness
237 Inventory” (SCI) (Berscheid et al., 1989), and the “We-scale” (Cialdini et al., 1997).
238 The IOS scale showed two circles increasingly overlapping labeled “You” and “X”, and
239 participants were given the following instructions: *Using the figure below select*
240 *which pair of circles best describes your relationship with this person. In the figure*
241 *“X” serves as a placeholder for the person shown in the image at the beginning of this*
242 *section, and you should think of “X” being that person. By selecting the appropriate*
243 *number please indicate to what extent you and this person are connected* (Aron et al.,
244 1992; Gächter et al., 2015). The SCI scale comprised the two following questions:
245 *Relative to all your other relationships (both same and opposite sex) how would you*
246 *characterize your relationship with the person shown at the beginning of this*
247 *section?*, and *Relative to what you know about other people's close relationships, how*
248 *would you characterize your relationship with the person shown at the beginning of*
249 *this section?* Participants responded with a number between one (*Not close at all*) and
250 seven (*Very close*) (Berscheid et al., 1989). The We-scale comprised the following
251 question: *Please select the appropriate number below to indicate to what extent you*
252 *would use the term “WE” to characterize you and the person shown at the beginning*
253 *of this section.* Participants responded with a number between one (*Not at all*) and
254 seven (*Very much so*). For each participant and each identity we created a composite
255 “familiarity score” by averaging the scores in the three scales.

256 We also introduced a scale aimed at estimating the amount of interaction or contact
257 between the participant and the target identity. The scale was based on the work by
258 Idson and Mischel (2001), and participants were asked to respond Yes/No to the
259 following six questions: *Have you ever seen him during a departmental event?*, *Have*
260 *you ever seen him during a party?*, *Have you ever had a group lunch/dinner/drinks*
261 *with him?*, *Have you ever had a one-on-one lunch/dinner/drinks with him?*, *Have*
262 *you ever texted him personally (not a group message)?*, and *Have you ever emailed*
263 *him personally (not a group email)?* The responses were converted to 0/1 and for each
264 participant and for each identity we created a “contact score” by summing all the
265 responses.

266 For each subject separately, to obtain a measure of familiarity and contact related to
267 each morph, we averaged the familiarity and contact scores of each pair of identities
268 (e.g., the familiarity score of morph *ab* was the average of the scores for identity *a* and
269 identity *b*).

270 *Psychometric fit*

271 For both experiments we fitted a group-level psychometric curve using Logit Mixed-
272 Effect models (Moscatelli et al., 2012) as implemented in *lme4* (Bates et al., 2015). For
273 each experiment and each session, we fitted a model of the form

$$274 \quad y^k = \text{logit} \left(\beta_0 x + \sum_{i=1}^n (\beta_i + z_i^k) I_i \right)$$

275 where k indicates the subject, n is the number of angular locations ($n = 8$ for the first
 276 experiment, and $n = 4$ for the second experiment), I_i is an indicator variable for the
 277 angular location, β_i are the model fixed-effects, and z_i are the subject-level random-
 278 effects (random intercept). From this model, we defined for each subject the Point of
 279 Subjective Equality (PSE) as the point x such that $\text{logit}(x) = 0.5$, that is for each angular
 280 location

$$281 \quad PSE_i^k = -\frac{\beta_i}{\beta_0} - \frac{z_i^k}{\beta_0} = PSE_i^p + \Delta PSE_i^k$$

282 Thus, the PSE for subject k at angular location i can be decomposed in a population-
 283 level PSE and a subject-specific deviation from the population level, indicated with
 284 PSE^p and ΔPSE^k respectively.

285 In Experiment 2 we fitted three separate models for each of the morph continua. In
 286 addition, prior to fitting we removed all trials in which subjects mistakenly reported
 287 a third identity. For example, if an image belonging to morph ab was presented, and
 288 subjects responded with c , the trial was removed.

289 To quantify the bias across locations, we computed a variance score by squaring the
 290 ΔPSE_i , and summing them across locations, that is $bias = \sum_{i=1}^4 (\Delta PSE_i)^2$. Because

291 this quantity is proportional to the variance against 0, throughout the manuscript we
292 refer to it as Δ PSE variance.

293 *Computational modeling*

294 To account for the retinotopic biases we simulated a population of neural units
295 activated according to the Compressive Spatial Summation model (Kay et al., 2013,
296 2015) and performed a model-based decoding analysis. This model was originally
297 developed as an encoding model (Naselaris et al., 2011) to predict BOLD responses
298 and estimate population receptive fields in visual areas and face-responsive areas such
299 as OFA, pFus, and mFus (Kay et al., 2015). We refer to activations of neural units that
300 can be thought as being voxels, small populations of neurons, or individual neurons.

301 The CSS model posits that the response of a neural unit is equal to

$$302 \quad r = g \cdot a^n$$

303 with $a = \int G(x, y | x_0, y_0, \sigma) S(x, y) dx dy$, and $G(x, y | x_0, y_0, \sigma)$ being a 2D gaussian
304 centered at x_0, y_0 , with covariance $\Sigma = \sigma I$, and $S(x, y)$ being the stimulus converted
305 into contrast map. The term g represents the gain of the response, while the power
306 exponent n accounts for subadditive responses (Kay et al., 2013).

307 We reanalyzed the data from the fMRI experiments in Kay et al. (2015) (*pRF-*
308 *estimation experiment* and *face-task experiment*) using the publicly available data
309 (<http://kendrickkay.net/vtcddata>) and code (<http://kendrickkay.net/socmodel/>) to

310 obtain parameter estimates for three ROIs (Inferior Occipital Gyrus, IOG—also
311 termed OFA—mFus, and pFus). The simulation results were similar using parameter
312 estimates from both experiments, thus we describe the procedure for the face-task
313 experiment only because of the similarities with the behavioral experiments reported
314 here. We refer the reader to their paper for more details on the experiments and data
315 preprocessing. In the face-task experiment three participants saw medium-sized faces
316 (3.2°) in 25 visual field locations (5x5 grid with 1.5° spacing), and were asked to
317 perform a 1-back repetition detection task on face identity while fixating at the center
318 of the screen. The resulting 25 betas were used to fit the models. As in the original
319 paper, negative beta estimates were rectified (set to 0) and the power exponent was
320 set to $n = 0.2$ and not optimized because of the reduced number of stimuli. Model
321 fitting was performed with cross-validation. Stimuli were randomly split into ten
322 groups, and each group was left out in turn for testing. The parameter estimates were
323 aggregated across cross-validation runs taking the median value.

324 We simulated a population of $N = N_a + N_b$ neural units, where N_a indicates the number
325 of units selective to identity a , and N_b indicates the number of units selective to
326 identity b . For simplicity we set $N_b = 1$ and varied N_a , effectively changing the ratio
327 of units selective to one of the two identities. We performed additional simulations
328 increasing the total number of units and found consistent results, but here we report
329 the simulation with $N_b = 1$ for simplicity and consistency with the hypothesis of small

330 neural populations responsive to specific identities. The stimuli consisted of contrast
331 circles of diameter 4° centered at 7° from the center, and placed at an angle of 45° ,
332 135° , 225° , and 315° , simulating Experiment 2. We simulated the activation of the
333 units assuming i.i.d. random noise normally distributed with mean of 0 and standard
334 deviation of 0.1.

335 Each experiment consisted of a learning phase in which we simulated the (noisy)
336 response to the full identities a and b in each of the four locations, with 10 trials for
337 each identity and location. We used these responses to train a Support Vector
338 Machine (Cortes and Vapnik, 1995) with linear kernel to differentiate between the
339 two identities based on the pattern of population responses. Then, we simulated the
340 actual experiment by generating responses to morphed faces. For simplicity, we
341 assumed a linear response between the amount of morphing and the population
342 response. That is, we assumed that if a morph with m percentage morphing towards
343 b was presented, the population response was a combination of the responses to a and
344 b , weighted by $(1-m, m)$. The amounts of morphing paralleled those used in the two
345 experiments (0, 17, 33, 50, 67, 83, 100). We simulated 10 trials for each angular
346 location and each amount of morphing, and recorded the responses of the trained
347 decoder. These responses were used to fit a logit model similar to the model used in
348 the main analyses (without random effects), and to estimate the Point of Subjective

349 Equality for each angular location. The sum of these squared estimates around 50%
350 was computed and stored.

351 We varied systematically the ratio N_a/N_b of units responsive to identity a , ranging
352 from 1 to 9, and repeated 500 experiments for each ratio. For each experiment,
353 parameter values (pRF location and size) were randomly sampled without
354 replacement from the population of parameters previously estimated from the face-
355 task experiment of Kay et al., 2015. We simulated attentional modulations by
356 modifying the gain for the units responsive to identity a between 1 and 4 in 0.5 steps,
357 and fixing the gain for identity b to 1. As an alternative, we simulated the effect of
358 increases in receptive field size for the units responsive to identity a by increasing
359 their receptive field size from 0% to 50% in 10% steps, while keeping the gain fixed
360 to 1. We simulated receptive fields in this way from three face-responsive ROIs (IOG,
361 mFus, and pFus).

362 *Code and data availability*

363 Code for the analyses, raw data for both experiments, single subject results, and
364 simulations are available at
365 https://osf.io/wdaxs/?view_only=28741ad9b640480a9af6b593ade1ebcf [temporary
366 private link for peer review: will be made public after publication], as well as
367 Extended Data.

368 **Results**369 *Experiment 1*

370 In this experiment, participants performed a two-alternative forced-choice (AFC) task
 371 on identity discrimination. In each trial they saw a face presented for 50 ms, and were
 372 asked to indicate which of the two identities they just saw. Each face could appear in
 373 one of eight stimulus locations. Participants performed the same experiment with the
 374 same task a second time, at least 33 days after the first session (average 35 days \pm 4
 375 days standard deviation).

376 Participants showed stable and idiosyncratic retinal heterogeneity for identification.
 377 The PSE estimates for the two sessions were significantly correlated (see Table 1 and
 378 Figure 2B), showing stable estimates, and the within-subject correlations of Δ PSEs
 379 (see Methods) was significantly higher than the between-subject correlation
 380 (correlation difference: 0.87 [0.64, 1.10], 95% BCa confidence intervals (Efron, 1987);
 381 see Table 2), showing that the biases were idiosyncratic (see Figure 2A for example
 382 fits for two different subjects).

Table 1. Correlation of parameter estimates across sessions for the two experiments.				
Parameter	r	t	df	p
Experiment 1				
PSE	0.89 [-0.23, 1]	4.86**	6	0.002831

Δ PSE	0.71 [0.47, 0.84]	5.47***	30	6.106e-06
Experiment 2				
PSE	0.98 [0.93, 0.99]	15.22***	10	3.042e-08
Δ PSE	0.64 [0.5, 0.75]	9.02***	118	3.997e-15
Note: All confidence intervals are 95% BCa with 10,000 repetitions. * $p < .05$. ** $p < .01$. *** $p < .001$				

383

Table 2. Comparison of within-subjects correlations of parameter estimates across sessions with between-subjects correlations.			
Morph	Within-subjects r	Between-subjects r	Difference
Experiment 1			
ab	0.65 [†] [0.57, 0.8]	-0.22 [-0.41, -0.01]	0.87 [†] [0.63, 1.1]
Experiment 2			
ab	0.32 [-0.10, 0.62]	-0.02 [-0.15, 0.11]	0.34 [-0.07, 0.69]
ac	0.62 [†] [0.35, 0.79]	-0.07 [-0.21, 0.08]	0.68 [†] [0.41, 0.92]
bc	0.85 [†] [0.61, 0.95]	-0.08 [-0.27, 0.12]	0.92 [†] [0.68, 1.15]
Note: All confidence intervals are 95% BCa with 10,000 repetitions. [†] indicates that the CIs do not contain 0.			

384

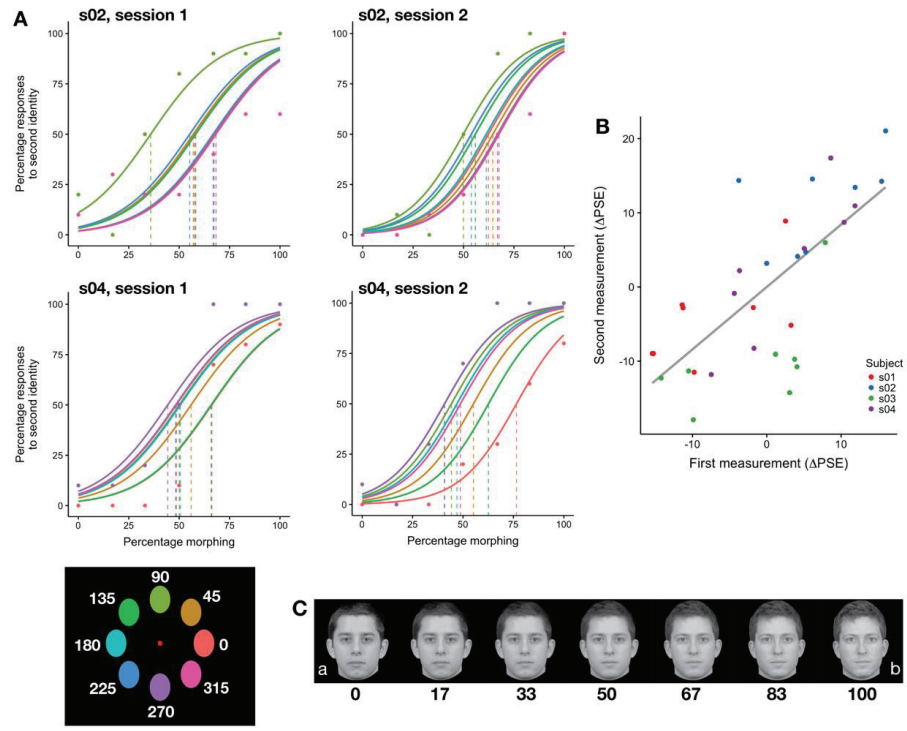


Figure 2. Stable and idiosyncratic biases in identification in Experiment 1. A) Psychometric fit for two subjects from both sessions. Colors indicate location (see colors in bottom left corner); actual data (points) are shown only for the extreme locations to avoid visual clutter. B) The parameter estimates across sessions (at least 33 days apart) were stable ($r = 0.71$ [0.47, 0.84], see Table 1). Dots represent individual parameter estimates for each location, color coded according to each subject. Correlations were performed on the data shown in this panel. C) Example morphs used in the experiment. Note that the morphs depicted here are shown for illustration only, and participants saw morphs of identities that were personally familiar to them.

385

386

387 ***Experiment 2***

388 In Experiment 1 participants exhibited stable, retinotopic biases for face identification
389 that were specific to each participant. Experiment 1, however, used only two target
390 identities, thus it could not address the question of whether the biases were specific
391 to target identities or to general variations in face recognition that would be the same
392 for all target faces. For this reason we conducted a second experiment in which we
393 increased the number of target identities. In Experiment 2, participants performed a
394 similar task as in Experiment 1 with the following differences. First, each face was
395 presented for 100 ms instead of 50 ms in order to make the task easier, since some
396 participants could not perform the task in Experiment 1; second, each face could
397 belong to one of three morphs, and participants were required to indicate which of
398 three identities the face belonged to; third, each face could appear in four retinal
399 locations instead of eight (see Figure 1) to maintain an appropriate duration of the
400 experiment. Each participant performed another experimental session at least 28 days
401 after the first session (average 33 days \pm 8 days SD).

402 We found that participants exhibited stable biases across sessions for the three morphs
403 (see Table 1 and Figure 3). Interestingly, within-subjects correlations were higher
404 than between-subjects correlations for the two morphs that included the identity *c*
405 (morphs *ac* and *bc*), but not for morph *ab* (see Table 2), suggesting stronger differences
406 in spatial heterogeneity caused by identity *c*. To test this further, we performed a two-

407 way ANOVA on the PSE estimates across sessions with participants and angular
408 locations as factors. The ANOVA was run for each pair of morphs containing the same
409 identity (e.g., for identity *a* the ANOVA was run on data from morphs *ab* and *ac*), and
410 the PSE estimates were transformed to be with respect to the same identity (e.g., for
411 identity *b* we considered PSE_{bc} and $100 - PSE_{ab}$). We found significant interactions
412 between participants and angular locations for identity *b* ($F(27, 120) = 1.77$, $p =$
413 0.01947) and identity *c* ($F(27, 120) = 3.34$, $p = 3.229e-06$), but not identity *a* ($F(27,$
414 $120) = 1.17$, $p = 0.2807$), confirming that participants showed increased spatial
415 heterogeneity for identities *b* and *c*. The increased spatial heterogeneity for identities
416 *b* and *c*, but not *a*, can be appreciated by inspecting the ΔPSE estimates for each
417 participant. Figure 4A shows lower bias across retinal locations for morph *ab* than the
418 other two morphs, suggesting more similar performance across locations for morph
419 *ab*. To investigate factors explaining the difference in performance across spatial
420 locations between the three identities, we compared the ΔPSE estimates with the
421 reported familiarity of the identities.

422 The variance of the average ΔPSE estimates across sessions for each subject was
423 significantly correlated with the reported familiarity of the identities
424 ($r = -0.56$ $[-0.71, -0.30]$, $t(28) = -3.59$, $p = 0.001248$), showing that the strength of the
425 retinal bias for identities was inversely modulated by personal familiarity (see Figure
426 4B). We estimated personal familiarity by averaging participants' ratings of the

427 identities on three scales (Inclusion of the Other in the Self, the We-Scale, and the
 428 Subjective Closeness Inventory, see Methods for details). The three scales were highly
 429 correlated (min correlation $r = 0.89$, max correlation $r = 0.96$).

430 Because the amount of personal familiarity was correlated with the amount of contact
 431 with a target identity ($r = 0.45$ [0.17, 0.68], $t(28) = 2.65$,
 432 $p = 0.01304$), we tested whether a linear model predicting Δ PSE with both contact
 433 and familiarity as predictors could fit the data better. Both models were significant,
 434 but the model with two predictors provided a significantly better fit ($X^2(1) = 6.30$, $p =$
 435 0.0121 , log-likelihood ratio test), and explained more variance as indicated by higher
 436 R^2 : $R^2 = 0.45$, adjusted $R^2 = 0.40$ for the model with both Familiarity and Contact scores
 437 ($F(2, 27) = 10.82$, $p = 0.0003539$), and $R^2 = 0.32$, adjusted $R^2 = 0.29$ for the model with
 438 the Familiarity score only ($F(1, 28) = 12.88$, $p = 0.001248$). Importantly, both
 439 predictors were significant (see Table 3), indicating that familiarity modulated the
 440 variance of the Δ PSE estimates in addition to modulation based on the amount of
 441 contact with a person. After adjusting for the contact score, the variance of the Δ PSE
 442 estimates and the familiarity score were still significantly correlated ($r_p = -0.42$ [-0.61,
 443 -0.16], $t(28) = -2.42$, $p = 0.02235$).

Table 3. Models predicting variance of the Δ PSE estimates across locations in Experiment 2.

Model	R^2	Score	β	η_p^2	t	p
-------	-------	-------	---------	------------	---	---

1	0.32	Familiarity	-0.0574	0.32	-3.59	0.0013
2	0.45	Familiarity	-0.0390	0.17	-2.38	0.0249
		Contact	-0.0452	0.19	-2.512	0.0183

444

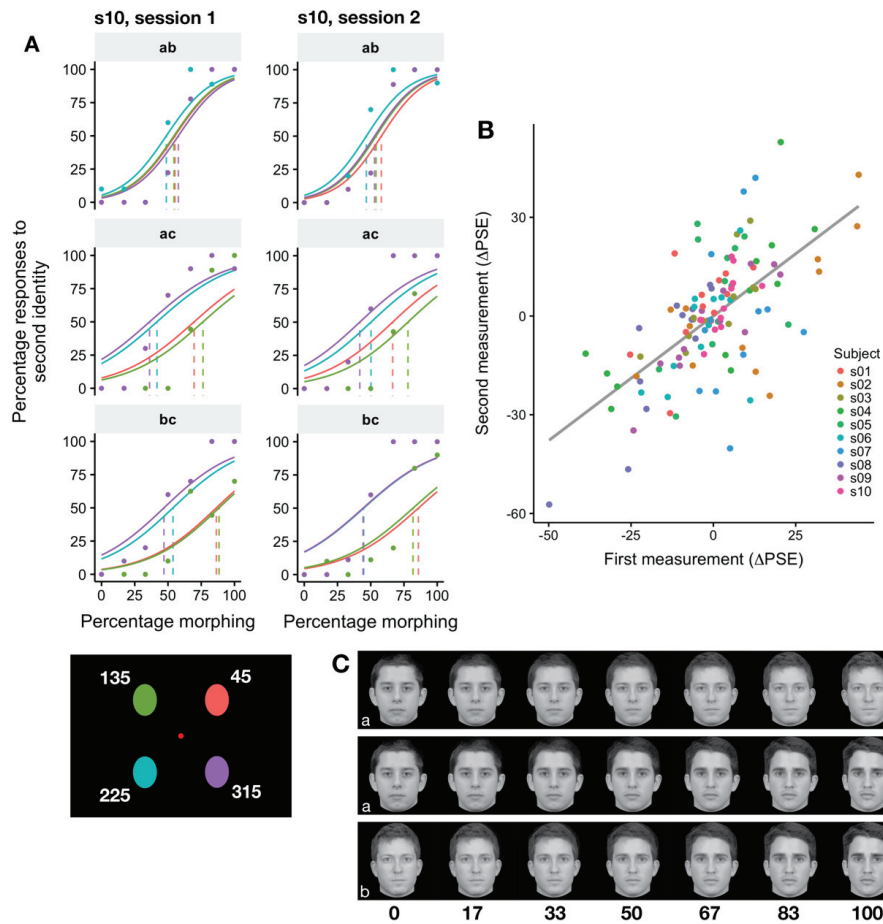


Figure 3. Stable and idiosyncratic biases in identification in Experiment 2. A) Psychometric fit for one subject from both sessions for each of the morphs. Colors indicate location (see colors in bottom left corner); actual data (points) are shown only for the extreme locations to avoid visual clutter. B) The parameter estimates across sessions (at least 28 days apart) were stable ($r = 0.64 [0.5, 0.75]$, see Table 1). Dots represent individual parameter estimates for each location, color coded

according to each participant. Correlations were performed on the data shown in this panel. C) Example morphs used in the experiment. Note that the morphs depicted here are shown only for illustration (participants saw morphs of identities who were personally familiar).

445

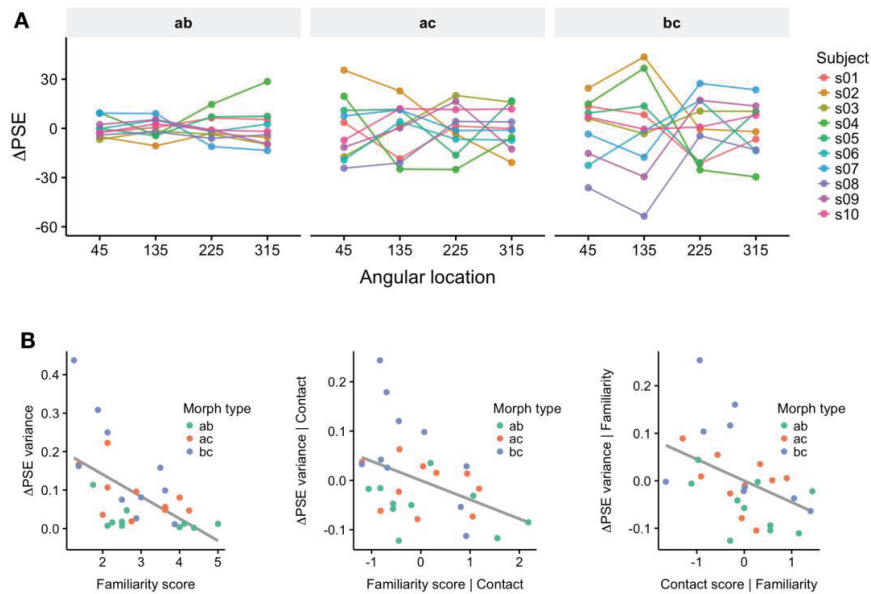


Figure 4. The strength of idiosyncratic biases was modulated by personal familiarity. A) Individual subjects' Δ PSE for each morph, averaged across sessions. Note the difference in variance across locations for the three different morphs (left to right)). B) The variance across locations of Δ PSE estimates was inversely correlated with the reported familiarity of the identities (left panel; $r = -0.56 [-0.71, -0.30]$), even when adjusting for the Contact score (middle panel; $r_p = -0.42 [-0.61, -0.16]$). The right panel shows the scatterplot between the Contact score and the Δ PSE variance, adjusted for the Familiarity score, which were significantly correlated as well ($r_p = -0.44 [-0.62, -0.17]$). See Methods for definition of the Familiarity score and the Contact score. Dots represent individual participant's data, color coded according to morph type. Correlations were performed on the data shown in these panels.

446

448 ***Model simulation***

449 In two behavioral experiments we found a stable, idiosyncratic bias towards specific
450 identities that varied according to the location in which the morphed face stimuli
451 appeared. The bias was reduced with more familiar identities, showing effects of
452 learning. To account for this effect, we hypothesized that small populations of
453 neurons selective to specific identities sample a limited portion of the visual field
454 (Afraz et al., 2010). We also hypothesized that with extended interactions with a
455 person, more neural units become selective to the facial appearance of the identity. In
456 turn, this increases the spatial extent of the field covered by the population and thus
457 reduces the retinotopic bias.

458 To quantitatively test this hypothesis, we simulated a population of neural units in
459 IOG (OFA), pFus, and mFus activated according to the Compressive Spatial
460 Summation model (Kay et al., 2013, 2015). The parameters of this model were
461 estimated from the publicly available data from Kay et al. (2015). We simulated
462 learning effects by progressively increasing the number of units selective to one of the
463 two identities, and measuring the response of a linear decoder trained to distinguish
464 between the two identities. As can be seen in Figure 5A, increasing the number of
465 units reduced the overall bias (expressed as variance against 0.5 of the PSE estimates,
466 see *Methods* for details) by increasing the spatial coverage (see Figure 5B).

467 Interestingly, the larger bias was found within the simulated IOG. Inspecting the pRF
468 coverage of the three ROIs revealed that the stimuli shown at 7° of eccentricity were
469 at the border of the receptive field coverage in IOG (Figure 5B) because of the smaller
470 RF sizes (median value across voxels of 2.98° [2.85°, 3.10°], 95% bootstrapped
471 confidence intervals), compared to those in pFus and mFus (3.87° [3.65°, 4.05°] and
472 3.55° [3.35°, 3.75°] respectively). To quantify this difference, we computed the
473 average proportion of units covering the stimulus locations in each ROI. As predicted
474 from the smaller RF sizes, fewer units in IOG covered the area where the stimuli were
475 presented (31.61%) compared to pFus (47.04%) and mFus (45.83%). These results
476 suggest that a larger retinotopic bias would be expected to originate from units in
477 IOG..

478 As alternative explanations, we tested whether differences in gain or increases in RF
479 size could reduce the bias to a similar extent as increasing the number of units. Figure
480 5C shows that modulating the gain failed to reduce the retinotopic bias in all
481 simulated ROIs, while Figure 5D shows that increasing RF size of the units responsive
482 to the more familiar identity can also reduce the retinotopic bias.

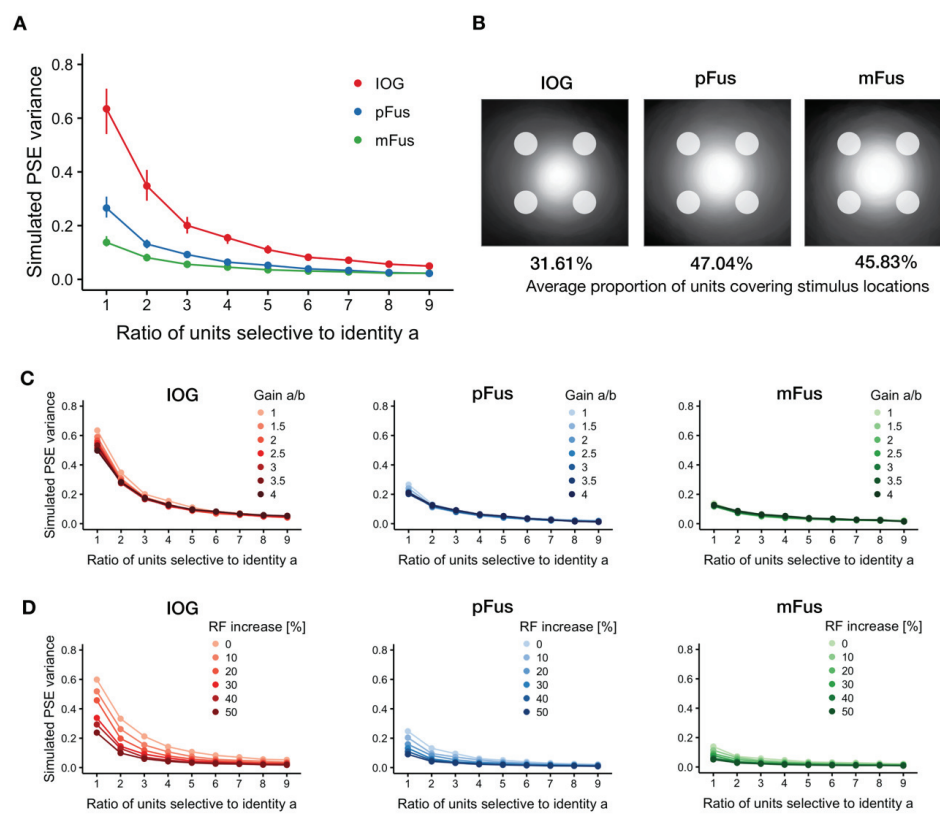


Figure 5. Simulating retinotopic biases and learning effects in face-responsive ROIs.

We hypothesized that neural units (voxels, small populations of neurons, or individual neurons) cover a limited portion of the visual field, and that learning increases the number of neural units selective to a particular identity. A) Increasing the number of units selective to one identity reduces the retinotopic bias. Results of simulating 500 experiments by varying the ratio of neural units selective to one of two identities and fixing the gain to 1 for both identities. Dots represent median values with 95% bootstrapped CIs (1,000 replicates; note that for some points the CIs are too small to be seen). In all simulated ROIs the variance of the PSE around 50% decreases with increasing number of units selective to *a*, but remains larger in IOG because of its receptive field size. B) Population coverage of the units in each ROI estimated from the face-task data in Kay et al. (2015) and used in the simulations. Circles at the periphery show the simulated stimulus locations. Each image is normalized to the number of units in each ROI. Receptive fields are computed with radius 2σ , following the convention in Kay et al., (2015). Percentages below each image show the average proportion of units whose receptive field cover the stimulus locations. Compared to pFus and mFus, fewer

units cover the stimuli in IOG resulting in a larger bias across locations. C) Increasing the gain of the response to one identity fails to reduce the retinotopic bias. D) Increasing the receptive field size of the units responsive to one identity reduces the retinotopic bias. In both C) and D) each dot represents median values of PSE variance for 500 simulated experiments. CIs are not shown to reduce visual clutter.

483

484 **Discussion**

485 Afraz et al. (2010) reported spatial heterogeneity for recognition of facial attributes
486 such as gender and age, suggesting that relatively independent neural populations
487 tuned to facial features might sample different regions of the visual field. Prolonged
488 social interactions with personally familiar faces lead to facilitated, prioritized
489 processing of those faces. Here we wanted to investigate if this learning of face
490 identity through repeated social interactions also affects these local visual processes,
491 by measuring spatial heterogeneity of identity recognition. We measured whether
492 face identification performance for personally familiar faces differed according to the
493 location in the visual field where face images were presented. We found that
494 participants exhibited idiosyncratic, retinotopic biases for different face identities that
495 were stable across experimental sessions. Importantly, the variability of the
496 retinotopic bias was reduced with increased familiarity with the target identities.
497 These data support the hypothesis that familiarity modulates processes in visual areas
498 with limited position invariance (Visconti di Oleggio Castello et al., 2017a).

499 These results extend the reports of spatial heterogeneity in visual processing to face
500 identification. Similar biases exist for high-level judgments such as face gender and
501 age (Afraz et al., 2010), as well as shape discrimination (Afraz et al., 2010), crowding,
502 and saccadic precision (Greenwood et al., 2017). Afraz et al. (2010) suggested that
503 neurons in IT exhibit biases that are dependent on retinal location because their
504 receptive field sizes are not large enough to provide complete translational invariance,
505 and stimuli in different locations will activate a limited group of neurons. In this work,
506 we show that these perceptual biases for face processing not only exist for gender and
507 age judgments (Afraz et al., 2010), but also for face identification and that these biases
508 are affected by learning.

509 *Location-dependent coding in face-responsive areas*

510 Neurons in temporal cortex involved in object recognition are widely thought to be
511 invariant to object translation, that is their response to an object will not be modulated
512 by the location of the object in the visual field (Riesenhuber and Poggio, 1999; Hung
513 et al., 2005). However, evidence suggests that location information is preserved in
514 activity of neurons throughout temporal cortex (Kravitz et al., 2008; Hong et al.,
515 2016). Location information can be encoded as a retinotopic map, such as in early
516 visual cortex, where neighboring neurons are selective to locations that are
517 neighboring in the visual field. In the absence of a clear cortical retinotopic map,
518 location information can still be preserved at the level of population responses

519 (Schwarzlose et al., 2008; Rajimehr et al., 2014; Henriksson et al., 2015; Kay et al.,
520 2015).

521 Areas of occipital and temporal cortices show responses to objects that are modulated
522 by position (Kravitz et al., 2008, 2010; Sayres and Grill-Spector, 2008). In particular,
523 also face-responsive areas of the ventral core system (Haxby et al., 2000; Visconti di
524 Oleggio Castello et al., 2017a) such as OFA, pFus, and mFus show responses that are
525 modulated by the position in which a face appears. Responses to a face are stronger in
526 these areas when faces are presented foveally rather than peripherally (Levy et al.,
527 2001; Hasson et al., 2002; Malach et al., 2002). In addition, early face processing areas
528 such as PL in monkeys or OFA in humans code specific features of faces in typical
529 locations. Neurons in PL are tuned to eyes in the contralateral hemifield, with
530 receptive fields covering the typical location of the eyes at fixation (Issa and DiCarlo,
531 2012). Similarly, OFA responses to face parts are stronger when they are presented in
532 typical locations (de Haas et al., 2016), and OFA activity codes the position and
533 relationship between face parts (Henriksson et al., 2015).

534 The modulation of responses by object location in these areas seems to be driven by
535 differences in receptive field sizes. In humans, population receptive fields (pRF) can
536 be estimated with fMRI by modeling voxel-wise BOLD responses (Dumoulin and
537 Wandell, 2008; Wandell and Winawer, 2011, 2015; Kay et al., 2013). These studies
538 have shown that pRF centers are mostly located in the contralateral hemifield (Kay

539 et al., 2015; Grill-Spector et al., 2017b), corresponding to the reported preference of
540 these areas for faces presented contralaterally (Hemond et al., 2007). In addition, pRF
541 sizes increase the higher in the face processing hierarchy, favoring perifoveal regions
542 (Kay et al., 2015; Silson et al., 2016). The location-dependent coding of faces in these
543 face-processing areas might be based on population activity, since these areas do not
544 overlap with retinotopic maps in humans (for example, OFA does not seem to overlap
545 with estimated retinotopic maps, Silson et al., 2016, but see Janssens et al., 2014;
546 Rajimehr et al., 2014; Arcaro and Livingstone, 2017; Arcaro et al., 2017 for work in
547 monkeys showing partial overlap between retinotopic maps and face patches).

548 *Cortical origin of idiosyncratic biases and effects of familiarity*

549 Populations of neurons in visual areas and in temporal cortex cover limited portions
550 of the visual field, with progressively larger receptive fields centered around
551 perifoveal regions (Grill-Spector et al., 2017b). This property suggests that biases in
552 high-level judgments of gender, age, and identity may be due to the variability of
553 feature detectors that cover limited portions of the visual field (Afraz et al., 2010).
554 While the results from our behavioral study cannot point to a precise location of the
555 cortical origin of these biases, our computational simulation suggests that a larger bias
556 could arise from responses in the OFA, given the estimates of receptive field size and
557 eccentricity in this area (Kay et al., 2015; Grill-Spector et al., 2017b). We cannot
558 exclude that this bias might originate in earlier areas of the visual processing stream.

559 In this work, we showed that the extent of variation in biases across retinal locations
560 was inversely correlated with the reported familiarity with individuals, suggesting
561 that a history of repeated interaction with a person may tune the responses of neurons
562 to that individual in different retinal locations, generating more homogeneous
563 responses. Repeated exposure to the faces of familiar individuals during real-life social
564 interactions results in a detailed representation of the visual appearance of a
565 personally familiar face. Our computational simulation suggests a simple process for
566 augmenting and strengthening the representation of a face. Learning through social
567 interactions might cause a greater number of neural units to become responsive to a
568 specific identity, thus covering a larger area of the visual field and reducing the
569 retinotopic biases. Our results showed that both ratings of familiarity and ratings of
570 amount of contact were strong predictors for reduced retinotopic bias; however,
571 familiarity still predicted the reduced bias when accounting for amount of contact.
572 While additional experiments are needed to test whether pure perceptual learning is
573 sufficient to reduce the retinotopic biases to the same extent as personal familiarity,
574 these results suggest that repeated personal interactions can strengthen neural
575 representations to a larger extent than mere increased frequency of exposure to a face.
576 This idea is consistent with neuroimaging studies showing a stronger and more
577 widespread activation for personally familiar faces compared to unfamiliar or
578 experimentally learned faces (Gobbini and Haxby, 2006; Cloutier et al., 2011; Natu

579 and O'Toole, 2011; Leibenluft et al., 2004; Gobbini and Haxby, 2007; Bobes et al.,
580 2013; Ramon and Gobbini, 2017; Visconti di Oleggio Castello et al., 2017a) .

581 *Effects of attention*

582 Could differences in attention explain the modulation of retinotopic biases reported
583 here? Faces, and personally familiar faces in particular, are important social stimuli
584 whose correct detection and processing affects social behavior (Brothers, 2002;
585 Gobbini and Haxby, 2007). Behavioral experiments from our lab have shown that
586 personally familiar faces break through faster in a continuous flash suppression
587 paradigm (Gobbini et al., 2013), and hold attention more strongly than unfamiliar
588 faces do in a Posner cueing paradigm (Chauhan et al., 2017). These results show that
589 familiar faces differ not only at the level of representations, but also in allocation of
590 attention. At the neural level, changes in attention might be implemented as increased
591 gain for salient stimuli or increased receptive field size (Kay et al., 2015). In an fMRI
592 experiment Kay et al. (2015) reported that population receptive field (pRF) estimates
593 were modulated by the type of task. Gain, eccentricity, and size of the pRFs increased
594 during a 1-back repetition detection task on facial identity as compared to a 1-back
595 task on digits presented foveally.

596 To address differences in gain in our computational simulation, we modified the
597 relative gain of units responsive to one of the two identities and found that it did not
598 influence the PSE bias across locations. This bias was more strongly modulated by the

599 number of units responsive to one of the identities. On the other hand, simulating
600 increases in receptive field size reduced the retinotopic bias almost as much as
601 increasing the number of units. These simulations suggest two alternative, and
602 possibly interacting, mechanisms that can reduce retinotopic biases in identification:
603 recruitment of additional units selective to an identity or changes in RF properties.
604 Additional experiments are needed to further characterize the differences in attention
605 and representations that contribute to the facilitated processing of personally familiar
606 faces.

607 *Implications for computational models of vision*

608 Many computational models of biological vision posit translational invariance:
609 neurons in IT are assumed to respond to the same extent, regardless of the object
610 position (Riesenhuber and Poggio, 1999; Serre et al., 2007; Kravitz et al., 2008). Even
611 the models that currently provide better fits to neural activity in IT such as
612 hierarchical, convolutional neural networks (Yamins et al., 2014; Kriegeskorte, 2015;
613 Yamins and DiCarlo, 2016) use weight sharing in convolutional layers to achieve
614 position invariance (LeCun et al., 2015; Schmidhuber, 2015; Goodfellow et al., 2016).
615 While this reduces complexity by limiting the number of parameters to be fitted,
616 neuroimaging and behavioral experiments have shown that translational invariance
617 in IT is preserved only for small displacements (DiCarlo and Maunsell, 2003; Kay et
618 al., 2015; Silson et al., 2016; for a review see Kravitz et al., 2008), with varying

619 receptive field sizes and eccentricities (Grill-Spector et al., 2017a). Our results
620 highlight the limited position invariance for high-level judgments such as identity,
621 and add to the known spatial heterogeneity for gender and age judgments (Afraz et
622 al., 2010). Our results also show that a higher degree of invariance can be achieved
623 through learning, as shown by the reduced bias for highly familiar faces. This finding
624 highlights that to increase biological plausibility of models of vision, differences in
625 eccentricity and receptive field size should be taken into account (Poggio et al., 2014),
626 as well as more dynamic effects such as changes induced by learning and attention
627 (Grill-Spector et al., 2017a).

628 *Conclusions*

629 Taken together, the results reported here support our hypothesis that facilitated
630 processing for personally familiar faces might be mediated by the development or
631 tuning of detectors for personally familiar faces in the visual pathway in areas that
632 still have localized analyses (Gobbini et al., 2013; Visconti di Oleggio Castello et al.,
633 2014, 2017b; Visconti di Oleggio Castello and Ida Gobbini, 2015). The OFA might be
634 a candidate for the cortical origin of these biases as well as for the development of
635 detectors for diagnostic fragments. Patterns of responses in OFA (and neurons in the
636 monkey putative homologue PL, Issa and DiCarlo, 2012) are tuned to typical locations
637 of face fragments (Henriksson et al., 2015; de Haas et al., 2016). Population receptive
638 fields of voxels in this region cover an area of the visual field that is large enough to

639 integrate features of intermediate complexity at an average conversational distance
640 (Kay et al., 2015; Grill-Spector et al., 2017b), such as combinations of eyes and
641 eyebrows, which have been shown to be theoretically optimal and highly informative
642 for object classification (Ullman et al., 2001, 2002; Ullman, 2007).

643 Future research is needed to further disambiguate differences in representations or
644 attention that generate these biases and how learning reduces them. Nonetheless, our
645 results suggest that prioritized processing for personally familiar faces may exist at
646 relatively early stages of the face processing hierarchy, as shown by the local biases
647 reported here. Learning associated with repeated personal interactions modifies the
648 representation of these faces, suggesting that personal familiarity affects face-
649 processing areas well after developmental critical periods (Arcaro et al., 2017;
650 Livingstone et al., 2017). We hypothesize that these differences may be one of the
651 mechanisms that underlies the known behavioral advantages for perception of
652 personally familiar faces (Burton et al., 1999; Gobbini and Haxby, 2007; Gobbini,
653 2010; Gobbini et al., 2013; Visconti di Oleggio Castello et al., 2014, 2017b; Ramon et
654 al., 2015; Visconti di Oleggio Castello and Gobbini, 2015; Chauhan et al., 2017; Ramon
655 and Gobbini, 2017).

656

657 **References**

- 658 Afraz A, Pashkam MV, Cavanagh P (2010) Spatial heterogeneity in the perception of
659 face and form attributes. *Curr Biol* 20:2112–2116.
- 660 Arcaro MJ, Livingstone MS (2017) A hierarchical, retinotopic proto-organization of
661 the primate visual system at birth. *Elife* 6
- 662 Arcaro MJ, Schade PF, Vincent JL, Ponce CR, Livingstone MS (2017) Seeing faces is
663 necessary for face-domain formation. *Nat Neurosci*
- 664 Aron A, Aron EN, Smollan D (1992) Inclusion of Other in the Self Scale and the
665 structure of interpersonal closeness. *J Pers Soc Psychol* 63:596.
- 666 Barragan-Jason G, Cauchoix M, Barbeau EJ (2015) The neural speed of familiar face
667 recognition. *Neuropsychologia* 75:390–401.
- 668 Bates D, Mächler M, Bolker B, Walker S (2015) Fitting Linear Mixed-Effects Models
669 Using lme4. *J Stat Softw* 67:1–48.
- 670 Berscheid E, Snyder M, Omoto AM (1989) The Relationship Closeness Inventory:
671 Assessing the closeness of interpersonal relationships. *J Pers Soc Psychol* 57:792.
- 672 Bobes MA, Lage Castellanos A, Quiñones I, García L, Valdes-Sosa M (2013) Timing
673 and tuning for familiarity of cortical responses to faces. *PLoS One* 8:e76100.
- 674 Brothers L (2002) The social brain: a project for integrating primate behavior and
675 neurophysiology in a new domain. *Foundations in social neuroscience*:367–
676 385.
- 677 Bruce V, Young A (1986) Understanding face recognition. *Br J Psychol* 77 (Pt 3):305–
678 327.
- 679 Burton AM, Wilson S, Cowan M, Bruce V (1999) Face Recognition in Poor-Quality
680 Video: Evidence From Security Surveillance. *Psychol Sci* 10:243–248.
- 681 Chauhan V, Visconti di Oleggio Castello M, Soltani A, Gobbini MI (2017) Social
682 Saliency of the Cue Slows Attention Shifts. *Front Psychol* 8:738.

- 683 Cialdini RB, Brown SL, Lewis BP, Luce C, Neuberg SL (1997) Reinterpreting the
684 empathy--altruism relationship: When one into one equals oneness. *J Pers Soc*
685 *Psychol* 73:481.
- 686 Cloutier J, Kelley WM, Heatherton TF (2011) The influence of perceptual and
687 knowledge-based familiarity on the neural substrates of face perception. *Soc*
688 *Neurosci* 6:63–75.
- 689 Cortes C, Vapnik V (1995) Support-vector networks. *Mach Learn* 20:273–297.
- 690 de Haas B, Schwarzkopf DS, Alvarez I, Lawson RP, Henriksson L, Kriegeskorte N,
691 Rees G (2016) Perception and Processing of Faces in the Human Brain Is Tuned
692 to Typical Feature Locations. *J Neurosci* 36:9289–9302.
- 693 Diamond R, Carey S (1986) Why faces are and are not special: An effect of expertise.
694 *J Exp Psychol Gen* 115:107.
- 695 DiCarlo JJ, Maunsell JHR (2003) Anterior inferotemporal neurons of monkeys
696 engaged in object recognition can be highly sensitive to object retinal position.
697 *J Neurophysiol* 89:3264–3278.
- 698 Dumoulin SO, Wandell BA (2008) Population receptive field estimates in human
699 visual cortex. *Neuroimage* 39:647–660.
- 700 Efron B (1987) Better Bootstrap Confidence Intervals. *J Am Stat Assoc* 82:171–185.
- 701 Faul F, Erdfelder E, Buchner A, Lang A-G (2009) Statistical power analyses using
702 G*Power 3.1: tests for correlation and regression analyses. *Behav Res Methods*
703 41:1149–1160.
- 704 Faul F, Erdfelder E, Lang A-G, Buchner A (2007) G*Power 3: a flexible statistical
705 power analysis program for the social, behavioral, and biomedical sciences.
706 *Behav Res Methods* 39:175–191.
- 707 Gächter S, Starmer C, Tufano F (2015) Measuring the Closeness of Relationships: A
708 Comprehensive Evaluation of the “Inclusion of the Other in the Self” Scale.
709 *PLoS One* 10:e0129478.

- 710 Gobbini MI (2010) Distributed process for retrieval of person knowledge. *Social*
711 *neuroscience: Toward understanding the underpinnings of the social mind*:40–
712 53.
- 713 Gobbini MI, Gors JD, Halchenko YO, Rogers C, Guntupalli JS, Hughes H, Cipolli C
714 (2013) Prioritized Detection of Personally Familiar Faces. *PLoS One* 8:e66620.
- 715 Gobbini MI, Haxby JV (2006) Neural response to the visual familiarity of faces. *Brain*
716 *Res Bull* 71:76–82.
- 717 Gobbini MI, Haxby JV (2007) Neural systems for recognition of familiar faces.
718 *Neuropsychologia* 45:32–41.
- 719 Goodfellow I, Bengio Y, Courville A, Bengio Y (2016) *Deep learning*. MIT press
720 Cambridge.
- 721 Greenwood JA, Szinte M, Sayim B, Cavanagh P (2017) Variations in crowding,
722 saccadic precision, and spatial localization reveal the shared topology of spatial
723 vision. *Proc Natl Acad Sci U S A* 114:E3573–E3582.
- 724 Grill-Spector K, Kay K, Weiner KS (2017a) The Functional Neuroanatomy of Face
725 Processing: Insights from Neuroimaging and Implications for Deep Learning.
726 In: *Deep Learning for Biometrics* (Bhanu B, Kumar A, eds), pp 3–31 *Advances*
727 *in Computer Vision and Pattern Recognition*. Cham: Springer International
728 Publishing.
- 729 Grill-Spector K, Weiner KS, Kay K, Gomez J (2017b) The Functional Neuroanatomy
730 of Human Face Perception. *Annu Rev Vis Sci* 3:167–196.
- 731 Guntupalli JS, Gobbini MI (2017) Reading Faces: From Features to Recognition.
732 *Trends Cogn Sci* 21:915–916.
- 733 Hasson U, Levy I, Behrmann M, Hendler T, Malach R (2002) Eccentricity bias as an
734 organizing principle for human high-order object areas. *Neuron* 34:479–490.
- 735 Haxby JV, Hoffman EA, Gobbini MI (2000) The distributed human neural system for
736 face perception. *Trends Cogn Sci* 4:223–233.
- 737 Hemond CC, Kanwisher NG, Op de Beeck HP (2007) A Preference for Contralateral
738 Stimuli in Human Object- and Face-Selective Cortex. *PLoS One* 2:e574.

- 739 Henriksson L, Mur M, Kriegeskorte N (2015) Faciotopy-A face-feature map with face-
740 like topology in the human occipital face area. *Cortex* 72:156–167.
- 741 Hong H, Yamins DLK, Majaj NJ, DiCarlo JJ (2016) Explicit information for category-
742 orthogonal object properties increases along the ventral stream. *Nat Neurosci*
743 19:613–622.
- 744 Hung CP, Kreiman G, Poggio T, DiCarlo JJ (2005) Fast readout of object identity from
745 macaque inferior temporal cortex. *Science* 310:863–866.
- 746 Idson LC, Mischel W (2001) The personality of familiar and significant people: the lay
747 perceiver as a social-cognitive theorist. *J Pers Soc Psychol* 80:585–596.
- 748 Issa EB, DiCarlo JJ (2012) Precedence of the Eye Region in Neural Processing of Faces.
749 *Journal of Neuroscience* 32:16666–16682.
- 750 Janssens T, Zhu Q, Popivanov ID, Vanduffel W (2014) Probabilistic and single-subject
751 retinotopic maps reveal the topographic organization of face patches in the
752 macaque cortex. *J Neurosci* 34:10156–10167.
- 753 Kay KN, Weiner KS, Grill-Spector K (2015) Attention reduces spatial uncertainty in
754 human ventral temporal cortex. *Curr Biol* 25:595–600.
- 755 Kay KN, Winawer J, Mezer A, Wandell BA (2013) Compressive spatial summation in
756 human visual cortex. *J Neurophysiol* 110:481–494.
- 757 Kleiner M, Brainard D, Pelli D, Ingling A, Murray R (2007) What's new in
758 Psychtoolbox-3. *Perception*
- 759 Kravitz DJ, Kriegeskorte N, Baker CI (2010) High-level visual object representations
760 are constrained by position. *Cereb Cortex* 20:2916–2925.
- 761 Kravitz DJ, Vinson LD, Baker CI (2008) How position dependent is visual object
762 recognition? *Trends Cogn Sci* 12:114–122.
- 763 Kriegeskorte N (2015) Deep Neural Networks: A New Framework for Modeling
764 Biological Vision and Brain Information Processing. *Annual Review of Vision*
765 Science 1:417–446.
- 766 LeCun Y, Bengio Y, Hinton G (2015) Deep learning. *Nature* 521:436–444.

- 767 Leibenluft E, Gobbini MI, Harrison T, Haxby JV (2004) Mothers' neural activation in
768 response to pictures of their children and other children. *Biol Psychiatry*
769 56:225–232.
- 770 Levy I, Hasson U, Avidan G, Hendler T, Malach R (2001) Center–periphery
771 organization of human object areas. *Nat Neurosci* 4:533–539.
- 772 Livingstone MS, Vincent JL, Arcaro MJ, Srihasam K, Schade PF, Savage T (2017)
773 Development of the macaque face-patch system. *Nat Commun* 8:14897.
- 774 Malach R, Levy I, Hasson U (2002) The topography of high-order human object areas.
775 *Trends Cogn Sci* 6:176–184.
- 776 Moscatelli A, Mezzetti M, Lacquaniti F (2012) Modeling psychophysical data at the
777 population-level: the generalized linear mixed model. *J Vis* 12
- 778 Naselaris T, Kay KN, Nishimoto S, Gallant JL (2011) Encoding and decoding in fMRI.
779 *Neuroimage* 56:400–410.
- 780 Natu V, O'Toole AJ (2011) The neural processing of familiar and unfamiliar faces: A
781 review and synopsis. *Br J Psychol* 102:726–747.
- 782 Poggio T, Mutch J, Isik L (2014) Computational role of eccentricity dependent cortical
783 magnification. *arXiv [csLG]*
- 784 Rajimehr R, Bilenko NY, Vanduffel W, Tootell RBH (2014) Retinotopy versus Face
785 Selectivity in Macaque Visual Cortex. *J Cogn Neurosci* 22:1–10.
- 786 Ramon M, Gobbini MI (2017) Familiarity matters: A review on prioritized processing
787 of personally familiar faces. *Vis cogn*:1–17.
- 788 Ramon M, Vizioli L, Liu-Shuang J, Rossion B (2015) Neural microgenesis of personally
789 familiar face recognition. *Proc Natl Acad Sci U S A* 112:E4835–E4844.
- 790 Riesenhuber M, Poggio T (1999) Hierarchical models of object recognition in cortex.
791 *Nat Neurosci* 2:1019–1025.
- 792 Sayres R, Grill-Spector K (2008) Relating retinotopic and object-selective responses
793 in human lateral occipital cortex. *J Neurophysiol* 100:249–267.

- 794 Schmidhuber J (2015) Deep learning in neural networks: An overview. *Neural Netw*
795 61:85–117.
- 796 Schwarzlose RF, Swisher JD, Dang S, Kanwisher N (2008) The distribution of category
797 and location information across object-selective regions in human visual cortex.
798 *Proc Natl Acad Sci U S A* 105:4447–4452.
- 799 Serre T, Oliva A, Poggio T (2007) A Feedforward Architecture Accounts for Rapid
800 Categorization. *Proc Natl Acad Sci U S A* 104:6424–6429.
- 801 Silson EH, Groen IIA, Kravitz DJ, Baker CI (2016) Evaluating the correspondence
802 between face-, scene-, and object-selectivity and retinotopic organization
803 within lateral occipitotemporal cortex. *J Vis* 16:14.
- 804 Sugiura M (2014) Neuroimaging studies on recognition of personally familiar people.
805 *Front Biosci* 19:672–686.
- 806 Taylor MJ, Arsalidou M, Bayless SJ, Morris D, Evans JW, Barbeau EJ (2009) Neural
807 correlates of personally familiar faces: parents, partner and own faces. *Hum*
808 *Brain Mapp* 30:2008–2020.
- 809 Ullman S (2007) Object recognition and segmentation by a fragment-based hierarchy.
810 *Trends Cogn Sci* 11:58–64.
- 811 Ullman S, Sali E, Vidal-Naquet M (2001) A Fragment-Based Approach to Object
812 Representation and Classification. In: *Visual Form 2001*, pp 85–100. Springer,
813 Berlin, Heidelberg.
- 814 Ullman S, Vidal-Naquet M, Sali E (2002) Visual features of intermediate complexity
815 and their use in classification. *Nat Neurosci*
- 816 Visconti di Oleggio Castello M, Guntupalli JS, Yang H, Gobbini MI (2014) Facilitated
817 detection of social cues conveyed by familiar faces. *Front Hum Neurosci* 8:678.
- 818 Visconti di Oleggio Castello M, Halchenko YO, Guntupalli JS, Gors JD, Gobbini MI
819 (2017a) The neural representation of personally familiar and unfamiliar faces in
820 the distributed system for face perception. *Sci Rep* 7:12237.
- 821 Visconti di Oleggio Castello M, Ida Gobbini M (2015) Familiar Face Detection in
822 180ms. *PLoS One* 10:e0136548.

- 823 Visconti di Oleggio Castello M, Wheeler KG, Cipolli C, Gobbini MI (2017b)
824 Familiarity facilitates feature-based face processing. *PLoS One* 12:e0178895.
- 825 Wandell BA, Winawer J (2011) Imaging retinotopic maps in the human brain. *Vision*
826 *Res* 51:718–737.
- 827 Wandell BA, Winawer J (2015) Computational neuroimaging and population
828 receptive fields. *Trends Cogn Sci* 19:349–357.
- 829 Willenbockel V, Sadr J, Fiset D, Horne GO, Gosselin F, Tanaka JW (2010) Controlling
830 low-level image properties: The SHINE toolbox. *Behav Res Methods* 42:671–
831 684.
- 832 Yamins DLK, DiCarlo JJ (2016) Using goal-driven deep learning models to understand
833 sensory cortex. *Nat Neurosci* 19:356–365.
- 834 Yamins DLK, Hong H, Cadieu CF, Solomon EA, Seibert D, DiCarlo JJ (2014)
835 Performance-optimized hierarchical models predict neural responses in higher
836 visual cortex. *Proc Natl Acad Sci U S A* 111:8619–8624.
- 837 Young AW, Burton AM (2017) Are We Face Experts? *Trends Cogn Sci*
838

839 Legends

840 **Figure 1. Experimental paradigm.** The left panel shows the experimental paradigm,
841 while the right panel shows the locations used in Experiment 1 (eight locations, top
842 panel) and in Experiment 2 (four locations, bottom panel).

843 **Figure 2. Stable and idiosyncratic biases in identification in Experiment 1.** A)
844 Psychometric fit for two subjects from both sessions. Colors indicate location (see
845 colors in bottom left corner); actual data (points) are shown only for the extreme
846 locations to avoid visual clutter. B) The parameter estimates across sessions (at least
847 33 days apart) were stable ($r = 0.71 [0.47, 0.84]$, see Table 1). Dots represent individual
848 parameter estimates for each location, color coded according to each subject.
849 Correlations were performed on the data shown in this panel. C) Example morphs
850 used in the experiment. Note that the morphs depicted here are shown for illustration
851 only, and participants saw morphs of identities that were personally familiar to them.

852 **Figure 3. Stable and idiosyncratic biases in identification in Experiment 2.** A)
853 Psychometric fit for one subject from both sessions for each of the morphs. Colors
854 indicate location (see colors in bottom left corner); actual data (points) are shown only
855 for the extreme locations to avoid visual clutter. B) The parameter estimates across
856 sessions (at least 28 days apart) were stable ($r = 0.64 [0.5, 0.75]$, see Table 1). Dots
857 represent individual parameter estimates for each location, color coded according to
858 each participant. Correlations were performed on the data shown in this panel. C)
859 Example morphs used in the experiment. Note that the morphs depicted here are
860 shown only for illustration (participants saw morphs of identities who were
861 personally familiar).

862 **Figure 4. The strength of idiosyncratic biases was modulated by personal familiarity.** A)
863 Individual subjects' Δ PSE for each morph, averaged across sessions. Note the
864 difference in variance across locations for the three different morphs (left to right)).
865 B) The variance across locations of Δ PSE estimates was inversely correlated with the
866 reported familiarity of the identities (left panel; $r = -0.56 [-0.71, -0.30]$), even when
867 adjusting for the Contact score (middle panel; $r_p = -0.42 [-0.61, -0.16]$). The right panel
868 shows the scatterplot between the Contact score and the Δ PSE variance, adjusted for
869 the Familiarity score, which were significantly correlated as well ($r_p = -0.44 [-0.62, -$
870 $0.17]$). See Methods for definition of the Familiarity score and the Contact score. Dots
871 represent individual participant's data, color coded according to morph type.
872 Correlations were performed on the data shown in these panels.

873 **Figure 5. Simulating retinotopic biases and learning effects in face-responsive ROIs.** We
874 hypothesized that neural units (voxels, small populations of neurons, or individual
875 neurons) cover a limited portion of the visual field, and that learning increases the

876 number of neural units selective to a particular identity. A) Increasing the number of
877 units selective to one identity reduces the retinotopic bias. Results of simulating 500
878 experiments by varying the ratio of neural units selective to one of two identities and
879 fixing the gain to 1 for both identities. Dots represent median values with 95%
880 bootstrapped CIs (1,000 replicates; note that for some points the CIs are too small to
881 be seen). In all simulated ROIs the variance of the PSE around 50% decreases with
882 increasing number of units selective to a , but remains larger in IOG because of its
883 receptive field size. B) Population coverage of the units in each ROI estimated from
884 the face-task data in Kay et al. (2015) and used in the simulations. Circles at the
885 periphery show the simulated stimulus locations. Each image is normalized to the
886 number of units in each ROI. Receptive fields are computed with radius 2σ , following
887 the convention in Kay et al., (2015). Percentages below each image show the average
888 proportion of units whose receptive field cover the stimulus locations. Compared to
889 pFus and mFus, fewer units cover the stimuli in IOG resulting in a larger bias across
890 locations. C) Increasing the gain of the response to one identity fails to reduce the
891 retinotopic bias. D) Increasing the receptive field size of the units responsive to one
892 identity reduces the retinotopic bias. In both C) and D) each dot represents median
893 values of PSE variance for 500 simulated experiments. CIs are not shown to reduce
894 visual clutter.

895 **Table 1.** Correlation of parameter estimates across sessions for the two experiments.

896 **Table 2.** Comparison of within-subjects correlations of parameter estimates across
897 sessions with between-subjects correlations.

898 **Table 3.** Models predicting variance of the Δ PSE estimates across angular locations in
899 Experiment 2.

900 **Extended Data.** The archive contains data from both experiments, as well as the
901 analysis scripts.

902

903 **Tables**

Table 1. Correlation of parameter estimates across sessions for the two experiments.			
Parameter	r	t	df
Experiment 1			
PSE	0.89 [-0.23, 1]	4.86**	6
Δ PSE	0.71 [0.47, 0.84]	5.47***	30
Experiment 2			
PSE	0.98 [0.93, 0.99]	15.22***	10
Δ PSE	0.64 [0.5, 0.75]	9.02***	118
Note: All confidence intervals are 95% BCa with 10,000 repetitions. * $p < .05$. ** $p < .01$. *** $p < .001$			

904

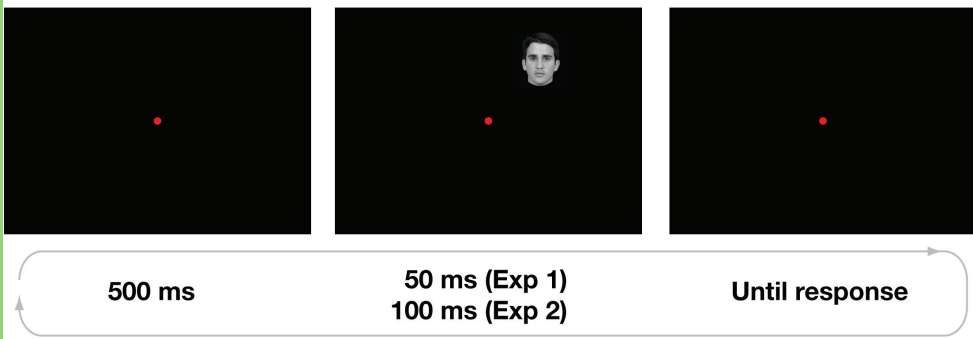
Table 2. Comparison of within-subjects correlations of parameter estimates across sessions with between-subjects correlations.			
Morph	Within-subjects r	Between-subjects r	Difference
Experiment 1			
ab	0.65 [†] [0.57, 0.8]	-0.22 [-0.41, -0.01]	0.87 [†] [0.63, 1.1]
Experiment 2			
ab	0.32 [-0.10, 0.62]	-0.02 [-0.15, 0.11]	0.34 [-0.07, 0.69]
ac	0.62 [†] [0.35, 0.79]	-0.07 [-0.21, 0.08]	0.68 [†] [0.41, 0.92]
bc	0.85 [†] [0.61, 0.95]	-0.08 [-0.27, 0.12]	0.92 [†] [0.68, 1.15]
Note: All confidence intervals are 95% BCa with 10,000 repetitions. [†] indicates that the CIs do not contain 0.			

905

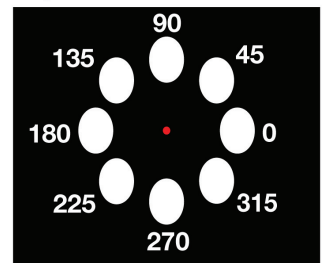
Table 3. Models predicting variance of the Δ PSE estimates across angular locations in Experiment 2.

Model	R ²	Score	β	η_p^2	t	p
1	0.32	Familiarity	-0.0574	0.32	-3.59	0.0013
2	0.45	Familiarity	-0.0390	0.17	-2.38	0.0249
		Contact	-0.0452	0.19	-2.512	0.0183

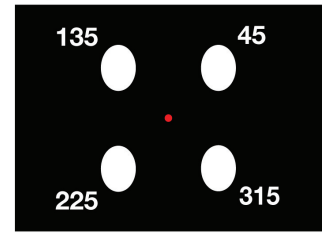
906



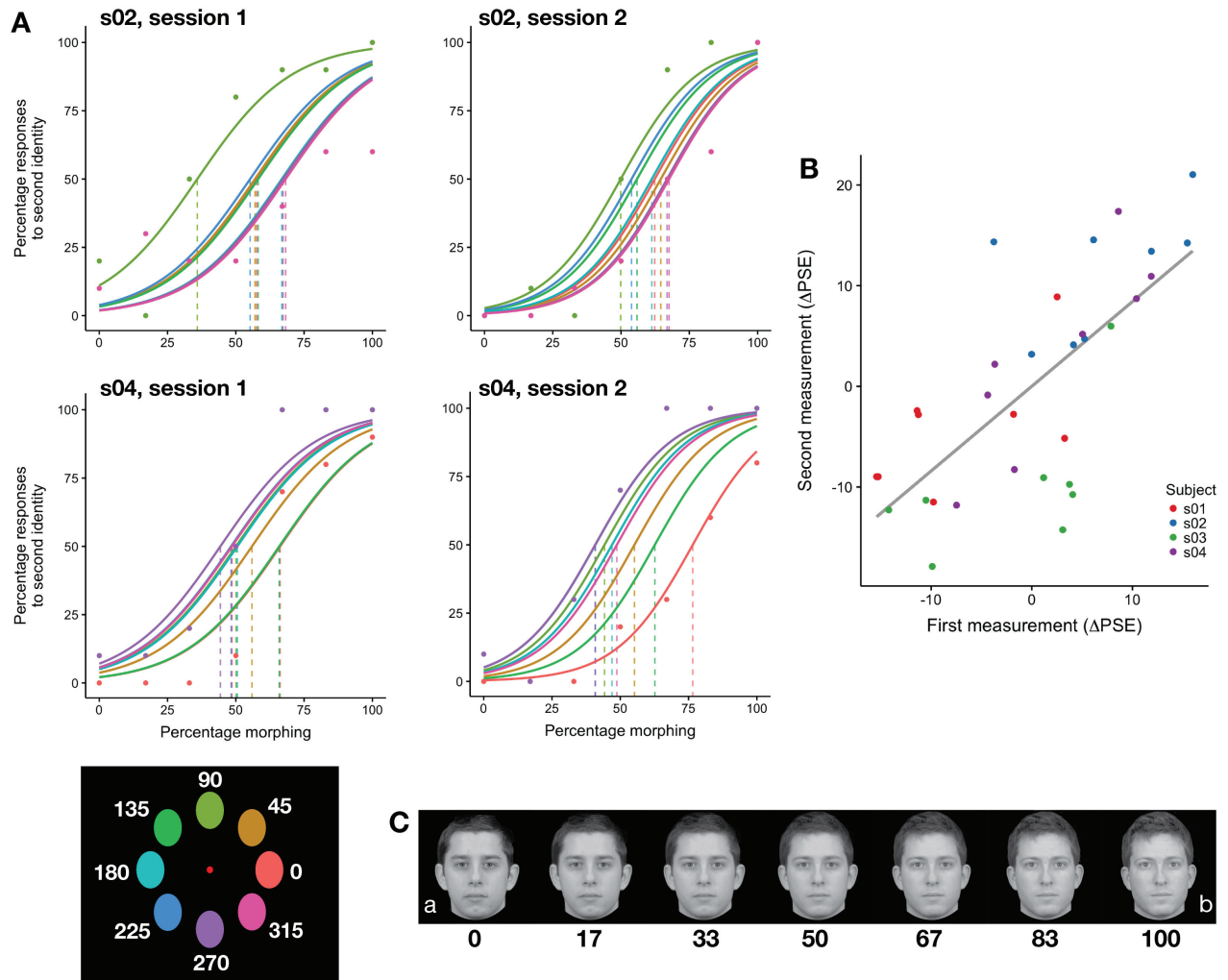
Exp 1

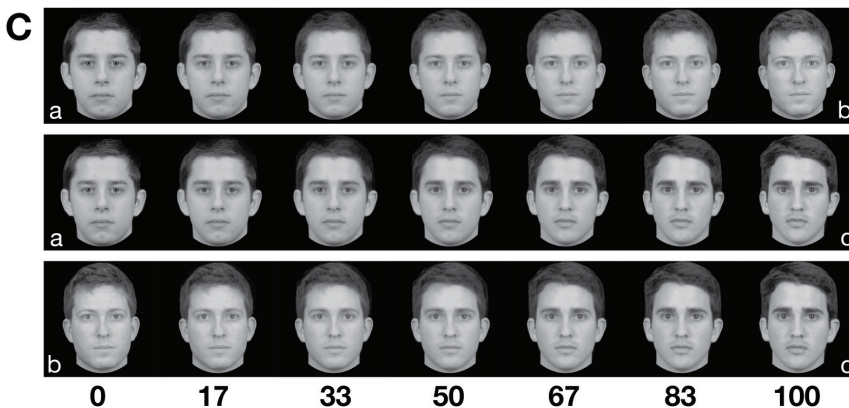
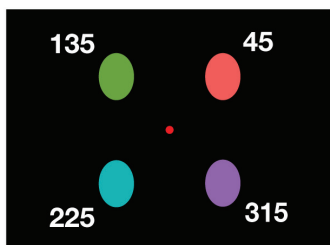
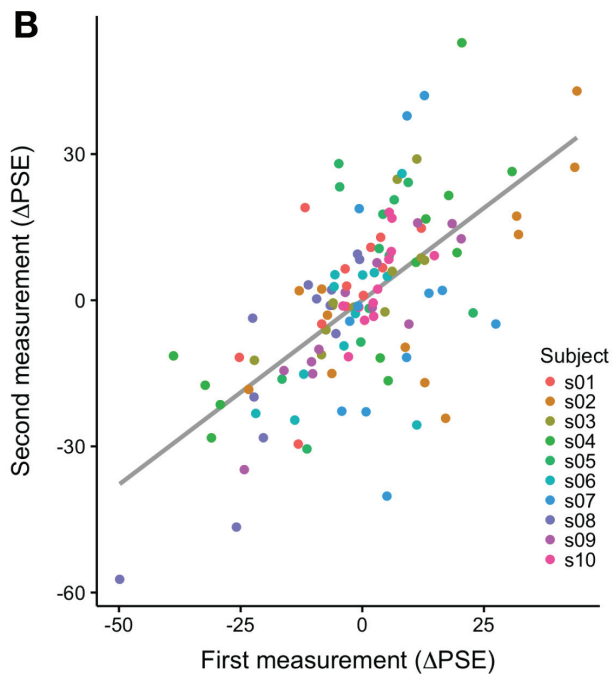
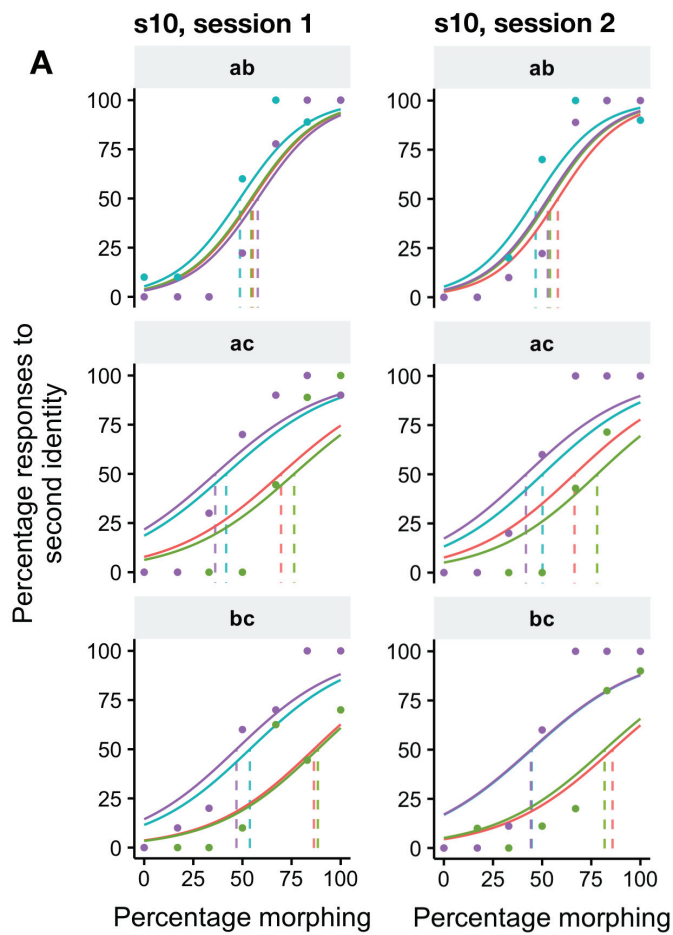


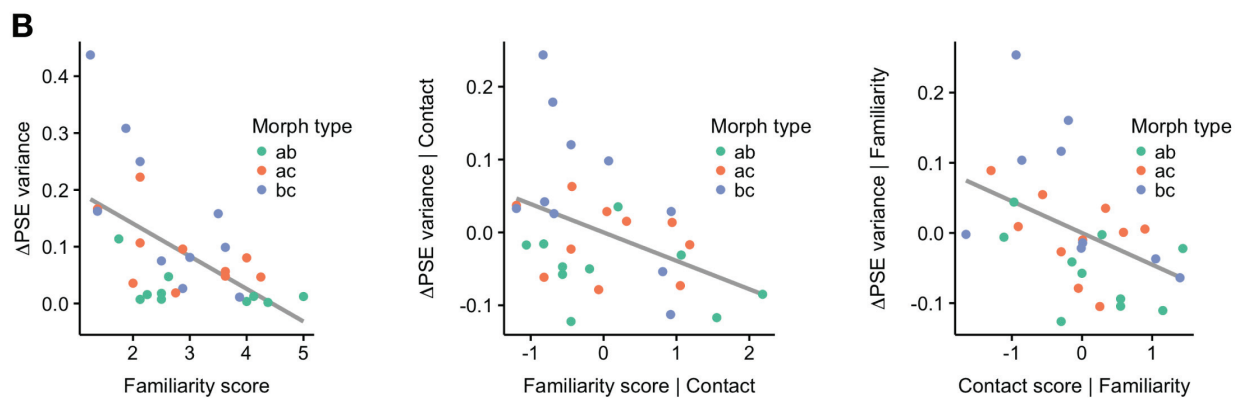
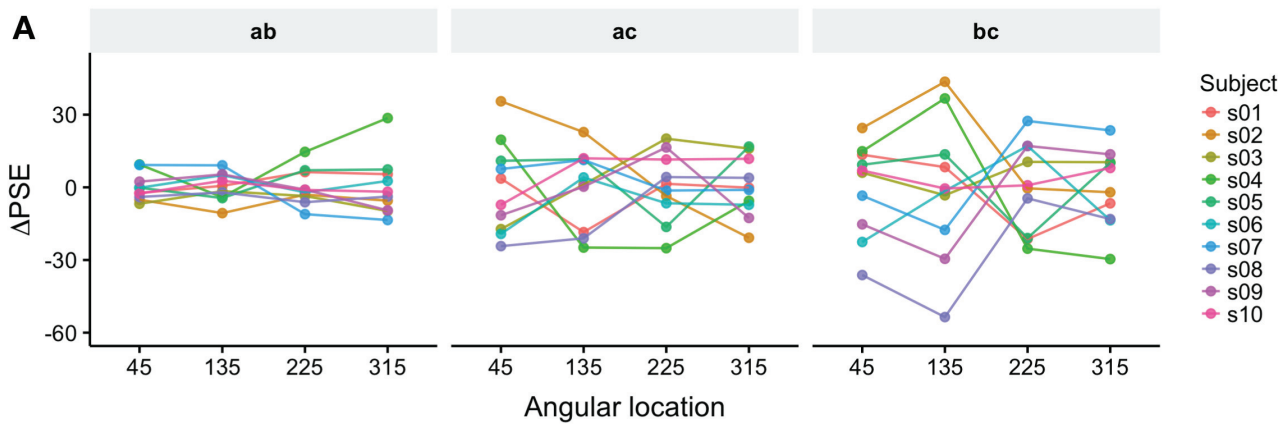
Exp 2



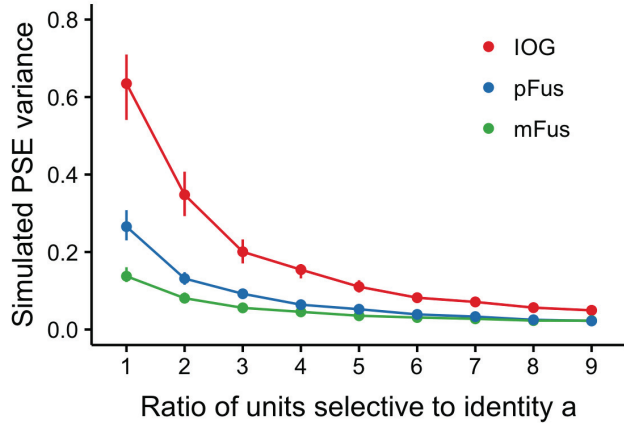
Stimulus locations



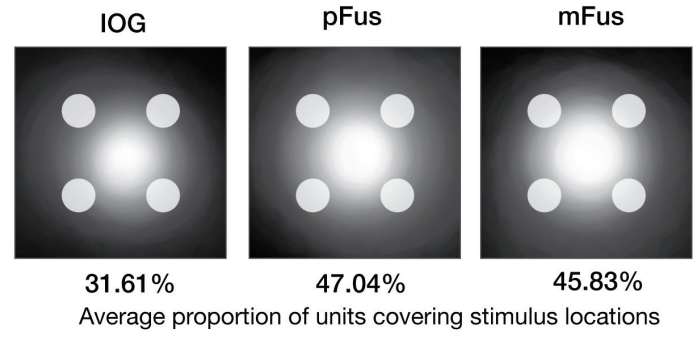




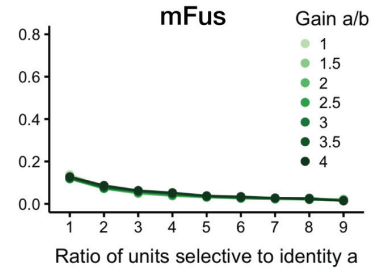
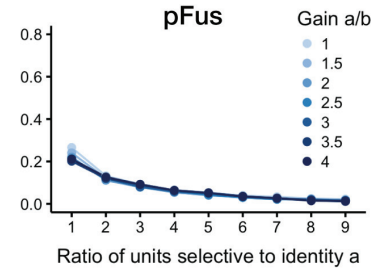
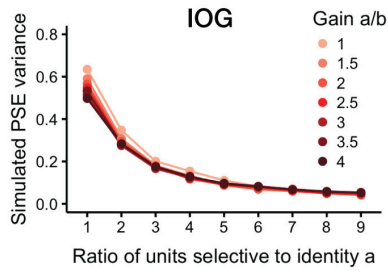
A



B



C



D

